Experimental characterization of the reaction-to-fire of an Acrylonitrile-Butadiene-Styrene (ABS) material using controlled atmosphere cone calorimeter

Fabien Hermouet, Thomas Rogaume, Eric Guillaume, Franck Richard, Damien Marquis, Xavier Ponticq

Version of Record: https://www.sciencedirect.com/science/article/pii/S0379711221000187
Manuscript_11020f5fdf60f8b56a8c9128b7777e0d

Experimental characterization of the reaction-to-fire of an Acrylonitrile-Butadiene-Styrene (ABS) material using Controlled Atmosphere Cone Calorimeter

Fabien Hermouet[1], Éric Guillaume[3], Thomas Rogaume[*,2], Franck Richard[2], Damien Marquis[4] & Xavier Ponticq[5]
1: Duorisk: Engineering, council and formation in fire safety, Poitiers, France
2: Institut P', UPR 3346 CNRS, Université de Poitiers, France
3: Efectis France, France
4: Laboratoire National de Métrologie et d'Essais, France
5: Centre d'Etude des TUnnels (CETU), France
*Corresponding author: thomas.rogaume@univ-poitiers.fr +33 682849288

ABSTRACT

Plastic materials are used increasingly in different domains and the comprehension of the phenomena occurring when they are exposed to a thermal stress has become a huge challenge over years. Indeed, an accurately described thermal decomposition of materials can help both, determining the conditions for which ignition can occur and evaluating their participation to a fire growth and propagation. Numerous parameters influence the thermal decomposition, especially the irradiance level and the local oxygen concentration of the environment where decomposition occurs.

The present paper deals with the assessment of the thermal behaviour of an Acrylonitrile-Butadiene-Styrene material, considering both phenomena occurring in condensed and gaseous phases. The results of Controlled Atmosphere Cone Calorimeter and Fourier Transform InfraRed spectrometer are presented for different test conditions (variation of the oxygen concentration environment and the irradiance levels imposed at the material surface). This study allows the determination of different combustion regimes depending on the oxygen concentration. It also highlights the effects of both the oxygen richness and the heat flux on the parameters which allow assessing the material's thermal behaviour: ignition time, mass loss rates, heat release rate and emissions of combustible and hazardous gaseous compounds.

KEYWORDS

Thermal decomposition, combustion regimes, FTIR, pyrolysis, mass loss rate, combustion conditions.

INTRODUCTION

The decomposition behaviour of polymeric materials strongly depends on the environment in which their decomposition is initiated. Above all parameters that can affect the decomposition process, two of them are particularly important to consider when studying the thermal behaviour of a specific material: the radiative heat flux received at the surface of the material and the local oxygen concentration.
Behind these two parameters and their effects on the phenomena that occurs in the condensed and the gaseous phases, are hidden numerous information about the development of a fire. Here therefore lies the interest of studying the thermal decomposition of polymeric materials in order to obtain knowledge on the prevention of enclosed fires.
A growing number of publications focus on results obtained using Controlled Atmosphere Cone Calorimeter (CACC) [1] to assess the fire behaviour and gaseous emissions of several materials [2–6].

However, only a few studies describe the thermal decomposition, on a large domain of irradiance level and oxygen concentration, in explaining the interactions between condensed and gaseous phases [7]. These interactions are of great interest because they allow to define decomposition material kinetics and its key parameters, and by extension, the development of a fire (growth, burning intensity, combustion limits, *etc.*).

In this context, this work deals with the complete assessment of the thermal behaviour of an Acrylonitrile-Butadiene-Styrene (ABS) material using a Controlled Atmosphere Cone Calorimeter [1] coupled to a Fourier Transform InfraRed (FTIR) spectrometer, in respect of [8].

Acrylonitrile butadiene styrene is a thermoplastic polymer which exhibits good mechanical strength while retaining a certain flexibility. It is therefore widely used. ABS is a two-phase material, manufactured by adding a polybutadiene-based elastomeric material to a Styrene Acrylonitrile (SAN) copolymer matrix. Due to its manufacture involving three monomers, it belongs to the terpolymer family and from a chemical point of view, its main chain therefore contains three repeating units. Its chemical formula is (C_8H_8-C_4H_6-C_3H_3N), so it predominantly contains carbon, hydrogen and nitrogen. However, it is often used with other compounds such as Bromine (Br) or Chlorine (Cl) to provide various functions such as resistance to fire, ultraviolet radiation, etc. There are thus grouped under the term ABS a multitude of materials of the same base, but slightly different due to these charges. The developed formulas of the ABS and of each of its constituents are given in Figure 1 [9].

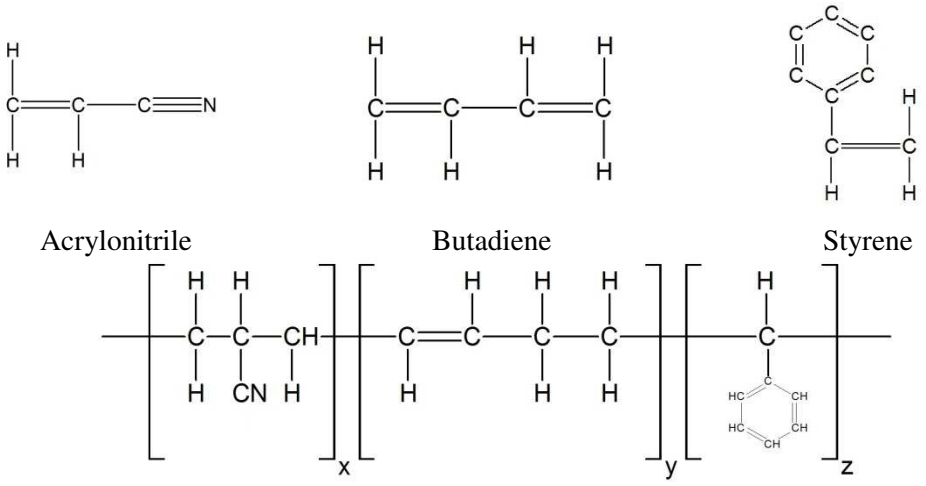

Figure 1: Developed formula of acrylonitrile, butadiene, and styrene and of ABS (From Vandome *[9]*).

Depending on the properties sought according to the use of ABS, the proportions of each constituent can be very different. For standard ABS, the mass percentages of the individual constituents are generally within the following ranges [9]:

- Acrylonitrile: 45 - 65%
- Butadiene: 10 - 28%
- Styrene: 10 - 35%

A great disparity therefore exists in the conception of this product. Thus, the physical, chemical and thermal properties of the ABS may differ depending on its final composition. This complicates the establishment of general rules on the thermal decomposition of this copolymer.

The thermal decomposition of ABS has been studied by several authors thanks to Thermogravimetric Analysis (ATG) under an inert atmosphere [10–13]. However, due to the almost systematic addition of other compounds to this product, it is difficult to describe in general the mechanisms associated with its thermal decomposition. From the conclusions of the various authors [10-13], the decomposition of

ABS is initiated at around 250 to 300°C and generally ends before reaching 500°C. The decomposition process is linked to the breaking of the bonds between the three monomers (butadiene, acrylonitrile and styrene) which are consecutively emitted as the temperature increases.
Furthermore, the entire mass is never degraded and an amount of residue representing approximately 5% of the initial mass remains at the end of the test. This residue is supposed to be the remaining mineral fillers classically added to the matrix to enhance the mechanical properties such as talc or silica.
Very little work has been carried out on a larger scale, in particular that of the cone calorimeter, and only some data on the rate of heat release and mass loss are available [14,15]. These two studies were carried out under the same conditions and use samples of 3 mm thickness subjected to an irradiance of 35 $kW.m^{-2}$ under an oxidizing atmosphere. Results show that the decomposition of the ABS under oxidizing atmosphere assessed using cone calorimeter occurs in a single phase. Moreover, the results obtained illustrate important differences, in particular concerning the duration of decomposition of the material and the rate of maximum heat release achieved. These dissimilarities can undoubtedly be attributed to differences in the contents of the components of ABS which are not specified by the authors.

In addition, Rutkowski & Levin [16] have attempted to synthesize available data to describe the toxicity of gaseous effluents associated with the thermal decomposition of ABS, under an oxidizing and inert atmosphere. Twenty-seven gaseous species can be identified during the decomposition of this material under an oxidizing atmosphere (against twenty under an inert atmosphere) including the polymers composing the terpolymer. This last information can be related to the work of Suzuki & Wilkie [12] which indicates that the three constituent monomers of ABS (Acrylonitrile, Butadiene and Styrene) are emitted successively as the temperature of the material increases.

In order to assess the thermal behaviour of the selected ABS material (described in the next section), 18 experimental conditions have been considered in order to deliver information on the decomposition of the material in drastically different decomposition environments. Thus, thanks to the controlled atmosphere cone calorimeter, the irradiance level imposed as the surface of the material as well as the oxygen concentration within the enclosure have been modified on a large range to assess the material thermal decomposition and the flammability limits. In this study, the irradiance level varies from 20 to 50 $kW.m^{-2}$ and oxygen concentration varies from 0 % [v/v] O_2 to ambient condition. The presented results concern ignition times, combustion regimes, Mass Loss Rates (MLR) and Heat Release Rate (HRR) evaluated under those different conditions. These results are cross-linked with qualitative and quantitative analysis of the gaseous emissions obtained thanks to a Fourier Transform InfraRed (FTIR) spectrometer.

MATERIAL AND EXPERIMENTAL PROTOCOL

Material description

The ABS tested in the present study is a commercial non flame retarded polymer whose exact composition is unknown. Details available on the material are presented hereafter:

- Producer: POLYPENCO
- Commercial designation: 42400104/3MM - PLASTIQUE ABS PLAQUE
- Colour: White
- Nominal Thickness: (3.00 ± 0.03) mm

ABS samples used are standard 100 mm by 100 mm in nominal thickness (3.0 mm). Their average mass is (32.09 ± 0.15 g). Backing condition is ensured by aluminum foil and silica wool (density of 64 $kg.m^{-3}$) as described in ISO 5660-1 standard [17]. These samples have been conditioned before test at (23 ± 2) °C and (50 ± 5) % RH for more than 88 hours in accordance with ISO 291 [18].

For each tested condition, experiments have been conducted at least three times to ensure the accuracy of the results in considering repeatability conditions according to ISO 5725 standard [19].

Presentation of the controlled atmosphere cone calorimeter apparatus (CACC)

The influence of the thermal decomposition parameters can be studied at small scale thanks to the CACC apparatus [1–7,20–24]. This test bench [1], presented in Figure 2, is composed of an enclosure fixed beneath the cone heater which constitutes the main difference comparing to the classical cone calorimeter described in ISO 5660-1 [17].

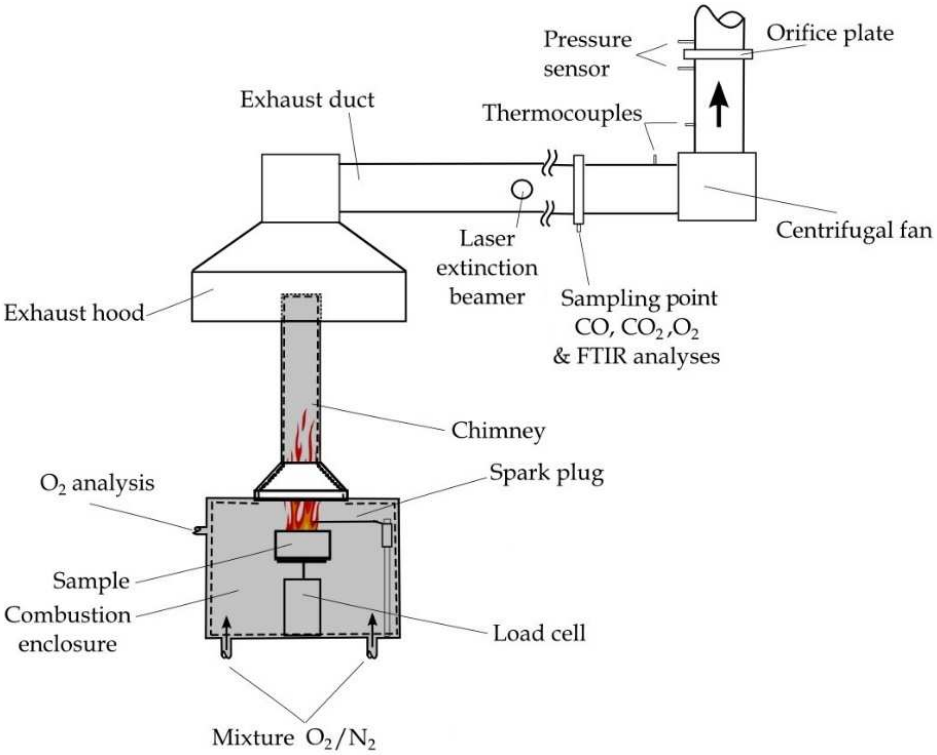

Figure 2 : Schematic representation of the controlled atmosphere cone calorimeter used

The enclosed box, which can be closed by a door, is equipped with two inlet ports at the bottom to inject the gaseous mixture composed of nitrogen and oxygen. The two gaseous compounds (Mixture O_2/N_2) are mixed upstream where the quantity of nitrogen and oxygen is controlled by two rotameters to ensure that the correct oxygen concentration is injected within the box at a sufficient flow rate. The flow rate must be controlled all along the experiments to prevent the vitiation of the atmosphere if too low, or the disturbance of the decomposition phenomenon if too high, as proven by Marquis *et al* [24]. According to this reference, the flow rate has been fixed to (160 ± 5) $L.min^{-1}$.

The oxygen concentration achieved in the box is besides permanently checked thanks to an oxygen analyzer, which allows accurate control of the mixture at a 2 $L.min^{-1}$ flow rate.

Above the cone heater, a 600 mm high stainless steel chimney has been fixed to the cone, in accordance ISO/TS 5660-5 [1] and ISO 13927 [25]. It prevents the diffusion of the ambient air in the enclosure, this may severely affect the local oxygen concentration at the surface of the sample by allowing a well ventilated decomposition environment. Other authors have already used this configuration to prevent this issue and thereby the post-oxidation of the gaseous effluents emitted by the combustion process [4,23,24]. As the chimney is leading gaseous compounds emitted during decomposition and combustion processes directly to ambient air, this configuration for the apparatus is classically referred as open CACC [23].

In this study, only piloted ignition is considered. Thus, tests have been performed using the spark ignitor prescribed for classical cone calorimeter [26].

The aforementioned adaptations to the classical cone calorimeter allow the study of thermal decomposition in well and under-ventilated environments. Using this apparatus, it is also possible to vary the irradiance level at the sample surface. The tested conditions for the present study concerns a domain from 20 to 50 kW.m^{-2}, with a 15 kW.m^{-2} step for the irradiance level, and from 0 to 21% [v/v] for the oxygen concentration. In all, 18 different conditions were studied as shown on Figure 3, where the red dots illustrate the tested oxygen concentration / irradiance level couples.

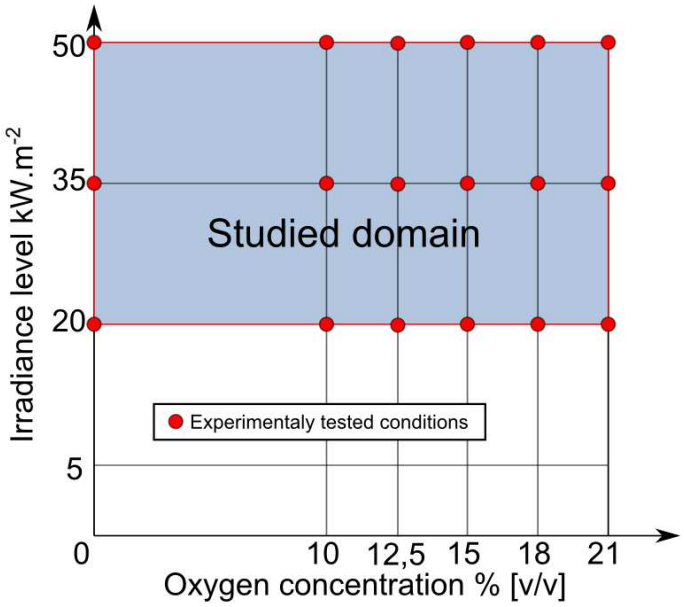

Figure 3: Tested conditions with Controlled Atmosphere Cone Calorimeter

The experimental procedure used is the following one: once the initial line data has been collected (CACC and gas analyzers), insert radiation shield in position, open enclosure door and remove the thermal barrier protecting the weighing device, then place the specimen holder and specimen on the weighing device and then close the enclosure door. The average time taken from opening to closing the enclosure door is about 10s. Thereafter, a delay of about 60s is necessary in order to reach the wanted O_2 concentration into the box (mixture O_2 / N_2). Upon stabilization, the test is initiated.

Heat release rate measurements

Oxygen consumption calorimetry, which is the most common method to measure HRR [27–29], is based on Thornton's findings [30]. According to this approach, most carbon-based combustibles (gas, liquid or solid) release a constant amount of energy for each unit mass of oxygen consumed during combustion. This energy is known as "*Thornton's constant*" and equal to 13.1 MJ.kg^{-1} oxygen consumed (± 5 % for most hydrocarbon fuels) [26,30].
For the standard cone calorimeter (according to the ISO 5660-1 standard [17]), the calculation of the HRR is based on Janssens' work [28,29]. Janssens published an algebraic method to calculate the HRR based on oxygen consumption. Based on Hess' Law, he derived a set of equations that address incomplete combustion by considering the generation of carbon monoxide. Unfortunately, the formula proposed by Janssens is not valid for the open CACC [5,23]. Due to its open design, the exhaust gases are diluted by excess air drawn from the laboratory environment. The excess air flow rate varies during a test, which affects the oxygen concentration baseline and hence the calculation of the HRR. Recently, Werrel [5,23] showed that the error from ignoring this effect can be as high as 30 % when the oxygen concentration in the enclosure is below 18 % [v/v]. Using Janssens's approach [28,29], Werrel defined a modified baseline and developed a new formula to calculate the HRR in the open CACC. Werrel's equations, which have been used in this paper to calculate the HRR, can be found in References [5,23].

Gas analysis

Gaseous effluents emitted during ABS decomposition process have been identified, then quantified with the help of a Horiba PG 250 and a FTIR which is one of the methodologies available for a continuous analysis of the fire effluents [8, 32-33]. The HORIBA PG250 gas analyzer is equipped with 3 detectors to quantify (in so many cases, relative uncertainty is in the range 5 – 10%): NO by chemiluminescence method (Limit of Quantification (LQ) ~ 5 µL.L-1), O_2 by electrochemical Zirconia method (LQ ~ 0.25% v/v) and CO_2, CO and SO_2 by NDIR absorption method (LQ ~ 0.08% v/v, ~ 12 µL.L-1 and ~ 9 µL.L-1, respectively) with a sampling flow rate equal to 0.4 $NL.min^{-1}$.

This apparatus is calibrated for fourteen gaseous compounds in different concentrations ranges listed in Table 1. Details on calibration and method validation are available in reference [33].

Calibrated Gases		**Detection limit ($\mu L.L^{-1}$)**	**Quantification limits ($\mu L.L^{-1}$)**
Gaseous compound	**Symbol**		
Carbon monoxide	CO	3	9-8802
Carbon dioxide	CO_2	60	180-50140
Nitrogen monoxide	NO	4	12-494
Nitrogen dioxide	NO_2	4	12-499
Nitrogen protoxide	N_2O	11	33-1005
Hydrogen cyanide	HCN	3	9-1020
Hydrogen chloride	HCl	4	12-5000
Methane	CH_4	12	36-4990
Acetylene	C_2H_2	1	3-994
Ethylene	C_2H_4	3	9-995
Formaldehyde	H_2CO	19	57-131
Sulfur dioxide	SO_2	5	15-852
Ammoniac	NH_3	1	3-1085

Table 1: List of the calibrated gaseous compounds and quantification limits of the FTIR used

During the experiments, effluents have been collected using a ring probe placed in the exhaust duct of the CACC (see Figure 2) at a flow rate of 2 $NL.min^{-1}$ during the FTIR measurements and 0,4 $NL.min^{-1}$ for the Horiba PG250 measurements. Effluents are transported using a heated sample line (180°C) to avoid gaseous compounds condensation. The disposition of the sampling point can be discussed as the gaseous compounds are sampled after being diluted in ambient air. Although the dilution factor is the same for all the test conditions, which allows comparisons between different test conditions, a post oxidation of the gaseous effluents can occur and might have an important effect at high heat flux (tests for which the temperature in the chimney and above is higher which enhances gases reactivity). Another bias can be considered as the gas thermal expansion coefficient may differ depending on the heat flux imposed at the surface of the material (temperature within the chimney and above) but this can be assumed to have a negligible effect on the results.
The sampling line has been connected to a filtration unit composed of two stainless steel heated filters of different dimensions (2 µm and 10 µm). After filtration, gases have been transported to a 2 L gas measurement cell with a 10 m optical path length. The spectrometer used for the analysis was a FTIR Thermo-Nicolet Magna IR 550 Series II equipped with a MCT-A detector. During the experiments, the data acquisition resolution has been set to 0.5 cm^{-1}. The pressure inside the gas cell has been regulated all along the test to be constant at 650 ± 10 torrs as prescribed in [35].

DETAILED ANALYSIS OF ABS THERMAL DECOMPOSITION

The main objective of this study has been to determine the fire behaviour of the ABS under different conditions as mentioned before. The typical cone calorimeter results are presented in this section: ignition time, mass loss rates, heat release rates and main gaseous species emitted during decomposition process. Thus, the presented results will focus mainly on the evolution of the decomposition kinetics of the material (depending on the combustion regime) and its effects on the gaseous emissions.

Experimental observations

Under an oxidative atmosphere, once exposed to the radiative heat flux imposed by the cone calorimeter, the thermal decomposition of the ABS material is initiated and pyrolysis gaseous compounds emerge from the surface of the material. Once the quantity of gaseous compounds emitted is sufficient, and if the oxygen concentration within the enclosure is also sufficient, ignition of the gaseous mixture occurs. As the flame appears locally near the spark ignitor, it rapidly spreads to the entire surface of the sample. Flame extinction can only be achieved when the totality of the material is consumed. At the end of the test, remains only whitish residues which are contained in the aluminum foil.
When the thermal decomposition intervenes without flame (below a certain oxygen concentration within the enclosure), the entire material is also consumed, although the residue physical appearance is very different in terms of coloring and structure. Indeed, at the end of the tests performed in such conditions, what remains in the sample holder is a blackish residue.
The observed difference in terms of residue obtained (highlighted by Figure 4) at the end of the tests indicates that the decomposition process is not similar when it takes place with or without a combustion process associated.

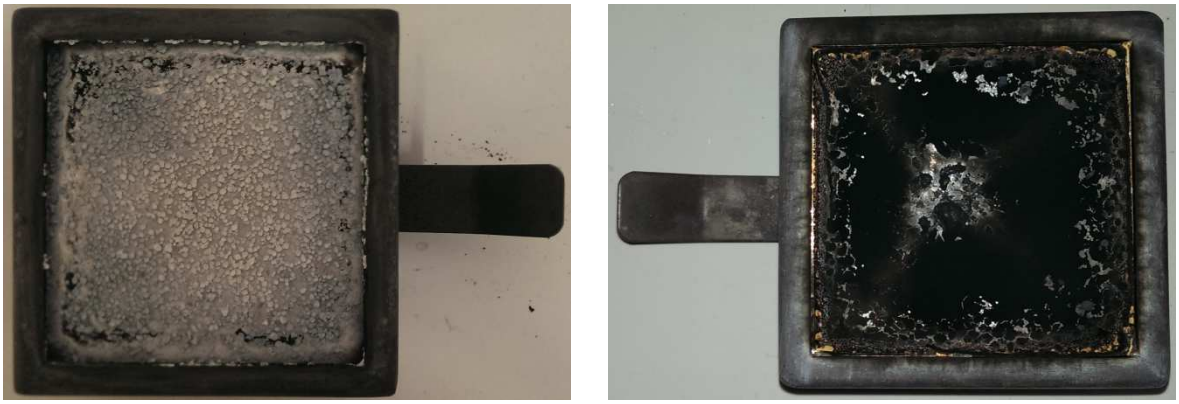

a) *b)*

Figure 4: Pictures of the ABS material after testing when the decomposition process is associated with a combustion process a) or flameless b).

Nonetheless, in any of the two cases described above, the material exhibits a particular behavior and even if it seems to be melting during the experiments, it does not expand or swell.

Time to ignition, combustion regimes and thermal response

One specific contribution of the study is to determine the impact of an oxygen depleted decomposition environment on the kinetic of thermal decomposition and of combustion. The first parameter of interest is the time-to-ignition of the material and by extension, the conditions in which a flame can appear. The experiments have all been conducted using the cone calorimeter spark ignitor above the surface of the material as prescribed in the classical cone calorimeter protocol [17]. Piloted time-to-ignition, for the different test conditions are presented in Table 2.

	Irradiance level		
Oxygen concentration	50 kW.m^{-2}	35 kW.m^{-2}	20 kW.m^{-2}
21 % [v/v]	(20.7 ± 1.5)	(39.0 ± 1)	(132.8 ± 17.4)
18 % [v/v]	(23.7 ± 1.2)	(52.7 ± 3.2)	(194.7 ± 19.2)
15 % [v/v]	(21.3 ± 1.5)	(42.0 ± 0.0)	(142.3 ± 15.6)
12.5 % [v/v]	(26.3 ± 2.5)	(51.7 ± 4.7)*	N.O.**

10 % [v/v]	N.O.**	N.O.**	N.O.**
0 % [v/v]	N.O.**	N.O.**	N.O.**
*Only flash points were observed **N.O.: Not Observed – Cases where no ignition occurred in at least 1200 s			

Table 2: Piloted ignition times of the studied ABS material for the different tested conditions (time in seconds)

As it can be seen in Table 2, reducing the heat flux at the surface of the material delays the ignition. Although, it's difficult to assess the effect of the reduction of the oxygen concentration within the enclosure on the ignition time, this reduction does not seem to have an effect whenever the irradiance level is fixed to 50 kW.m^{-2}. But differences in ignition times are observed thenceforth the energy transmitted to the material surface decreases (i.e. lower irradiance levels).

The plot of inverse of square root of ignition time vs. incident irradiance (Figure 5 *a)*) allows calculation the Thermal Response Parameter (TRP) of the material (as the inverse of the slope), as proposed by Tewarson [36] who expressed the link between this TRP, ignition temperature and thermal effusivity as: $TRP \sim (T_{ig} - T_0)\sqrt{k\rho c}$. Resulting values are compatible independently from oxygen concentration if ignition occurs. This means that thermal effusivity as well as ignition temperature are independent from the oxygen concentration if there is a sufficient amount of oxygen to allow ignition. The values of TRP found are in the range 223-226 kW.s$^{1/2}$.m² for oxygen concentrations between ambient and 15%. This might be compared to the value indicated by Tewarson [36] for ABS as 317 kW.s$^{1/2}$.m², indicating a large difference in the materials studied. As the material studied here is relatively thin, backing condition may have a great thermal impact. Please also note that Tewarson didn't give any details on sample thickness he studied in reference [36].

Figure 6 *b)* presents the total energy received by the specimen when ignition occurs for oxygen concentrations of 21 and 18% [v/v] O_2. This parameter has been calculated very simply in multiplying the heat flux imposed at the surface material by the ignition delay. Although this simple calculation is questionable because it does not consider the energy balance (i.e. the energetic loss due to convective, radiative and conductive processes), it provides useful pieces of information on the effects of oxygen concentration and cone calorimeter heat flux on ignition times. It especially highlights that the lower are the incident irradiance and the oxygen concentration, the higher is the amount of heat needed for ignition to occur.

In absence of measurement points for low irradiances, no interpretation is proposed on critical heat flux. Nevertheless, a test has been performed under air with an irradiance level of 13.5 kW/m². No ignition occurred in 1850 s, so the experimental critical heat flux is in the range [13.5 – 20] kW/m² under air. The theoretical value deduced as the intercept with x-axis from Figure 5 *a)* is not relevant. This means that backing boundary condition drives the ignition of this material at this thickness, in the specified test conditions. Tewarson [36] proposes a value between 9 and 15 kW.m^{-2} for this specific material which is in accordance with the one defined approximately in this study.

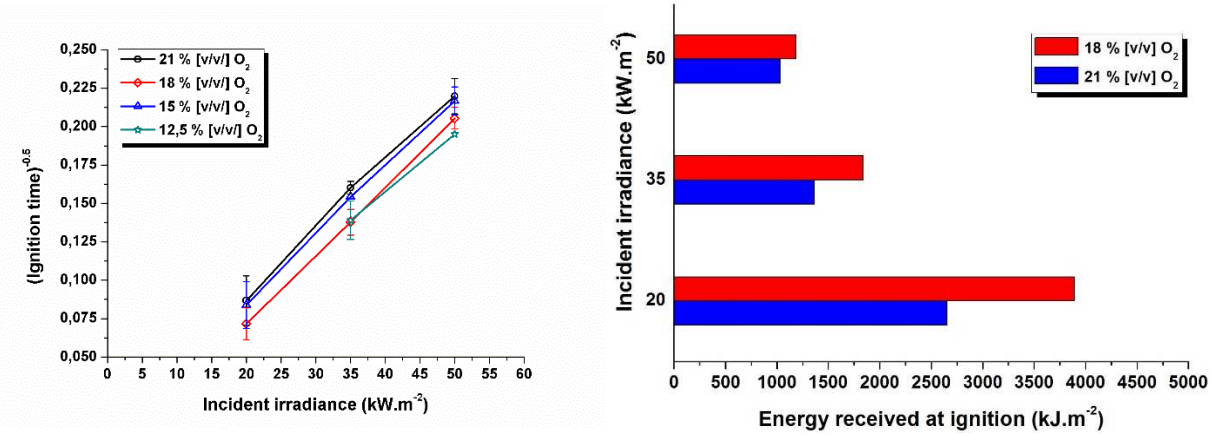

a) Discretized ignition time as function of incident heat flux *b) Energy received at ignition*

Figure 5: Ignition times and energie:

Besides, as expected, ignition does not occur for certain conditions. These conditions are in the range where oxygen concentration is a limiting factor for the combustion process. As a matter of fact, four conditions are needed for a sustainable combustion to occur:

1. A mass loss rate from the sample sufficient to produce enough gaseous fuel at the surface.
2. A ratio oxygen/fuel between lower and upper limits of flammability, which implies also a sufficient oxygen concentration.
3. Adequate mixing conditions of oxygen and air at the location of cone spark igniter.
4. Residence time compatible with ignition – this last condition is supposed to be reached as travel times are small enough around the igniter in comparison with ignition delays expected in the order of magnitude of tens to hundreds microseconds [37].

During this study, three main regimes have been observed: a well ventilated one, an under ventilated one andone corresponding to the transition between the first and the last.
More precisely, this regime corresponds to the transition between well ventilated and under ventilated regime and can be dissociated into three sub regimes. These regimes are illustrated schematically in Figure 6 and are described hereafter.

1. The first one (a) corresponds to a well-ventilated decomposition environment where a classical diffusion flame appears at the surface of the material.
2. The second one (b) corresponds to the achievement of the transition between well and under-ventilated conditions. Several phenomena can be observed in this transition phase but two specific cases have been observed numerous times for the ABS material:
    a. In the first case (c), ignition is not observed, although a succession of flash points are observed near the spark igniter. Indeed gaseous combustibles ignite locally without reaching a fire point and thus, the appearance of a well-established diffusion flame.
    b. In the second case (d), ignition occurs but not directly at the surface of the sample. Indeed it occurs within the chimney where the ventilation conditions are drastically modified compared to the ones found locally at the surface of the material. Stoichiometry between combustibles gaseous effluents and oxygen is achieved downstream and the mixture ignites within the chimney. This phenomenon has already been observed in reference [6]. Practically, this condition can only be encountered when the temperature in the chimney is high enough to ignite the mixture and does not happen when the irradiance level is too low (20 $kW.m^{-2}$). Another configuration, slightly different, can also be observed where ignition is observed at the outlet of the chimney. In this case, the regime can be qualified as a well ventilated one, as the oxygen concentration at the outlet of the chimney is that of ambient air (21% [v/v]).
3. Finally, the last one (e) corresponds to the achievement of the lower combustion limit and thus no ignition phenomena of any aforementioned types can be observed.

These regimes are described in Figure 6. For each, the figure is completed in order to determine if:

- The initially prescribed heat flux ($\dot{Q}_i^{''}$) must be completed or not by a component which represents the flame heat flux.
- The mass loss rate is supposed to be corrected because of the evolution of the total heat flux received due to the flame.

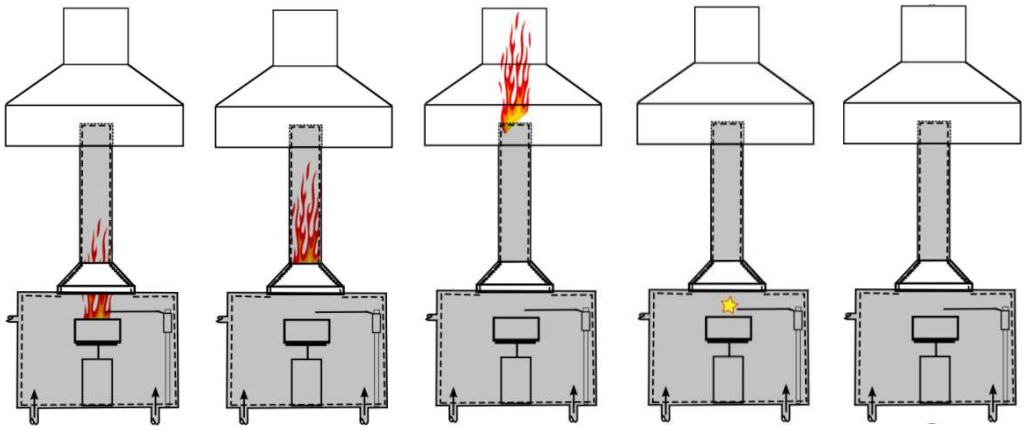

a) *b)* *c)* *d)* *e)*

Irradiance level	$> \dot{Q}_i''$	$> \dot{Q}_i''$	$\sim \dot{Q}_i''$	$\sim \dot{Q}_i''$	$\sim \dot{Q}_i''$
Mass Loss Rate	*Need of a correction*	*Need of a correction*	*Directly usable at a higher scale*	*Directly usable at a higher scale*	*Directly usable at a higher scale*

Figure 6: Decomposition regimes observed in CACC experiments

It might be noted that results may be highly dependent on mixing conditions, especially around spark ignitor. This means that results shall be analyzed in detail before any transposition outside the cone calorimeter design context. This point is particularly true for the gaseous emissions which, because of the open design of the CACC, cannot be used at a higher scale in any case (because they are dependent on the specific conditions of combustion met in the present CACC).

From this analysis, it is possible to define, as illustrated by Figure 7, a transition area between well and under ventilated decomposition conditions. The different combustion regimes can be found on the figure (illustrated by the numbers) which is just presented here for information (the limits presented are indicative and based on the experimental observations). A precise definition of the limits, even if it constitutes an interesting challenge, hides a huge experimental work.

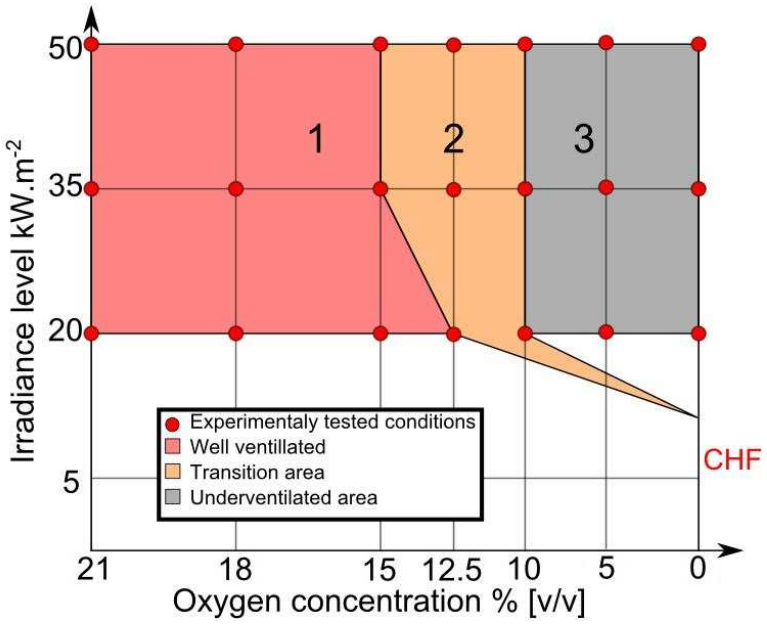

Figure 7: Example of the evolution of the combustion limits

**CHF: Critical Heat Flux (or minimum heat flux) – reference value according to Tewarson in SFPE Handbook* [36]*: 9-15 kW.m^{-2}*

It is a huge challenge to determine the combustion limits for a material as they clearly depend on the oxygen concentration but also of the irradiance level and mixing conditions due to test apparatus design. Indeed, even if the oxygen concentration can be sufficient to observe a combustion occurring

at the surface of the material, the quantity of combustible gaseous products available can also be a limiting factor. This last point explains why the limits of the combustion regimes are modified by reducing the irradiance level at the surface material until reaching a lower limit: the Critical Heat Flux (CHF; or minimum heat flux) (See Figure 7). The minimum heat flux is given here on the basis of previous studies that have shown that for the ABS material it is in the range of 9-15 kW.m^{-2} [36].

Mass loss rates

In this section, mass loss rates are presented for the different conditions considered during the experimental campaign. It is obvious, regarding the obtained results, that both irradiance level and oxygen concentration have an important effect on the decomposition kinetics as it can be seen in the graphs of Figure 8 (The graphs are voluntarily not presented on the same time scale for legibility purposes). All curves are presented without their relative errors to ensure legibility of the graphs, although the mean relative error for the presented MLR was determined to be approximately 2.5%. Data has been treated with a numerical filter (Savitzky-Golay smoothing) to limit experimental noise, as presented in [38] for details.

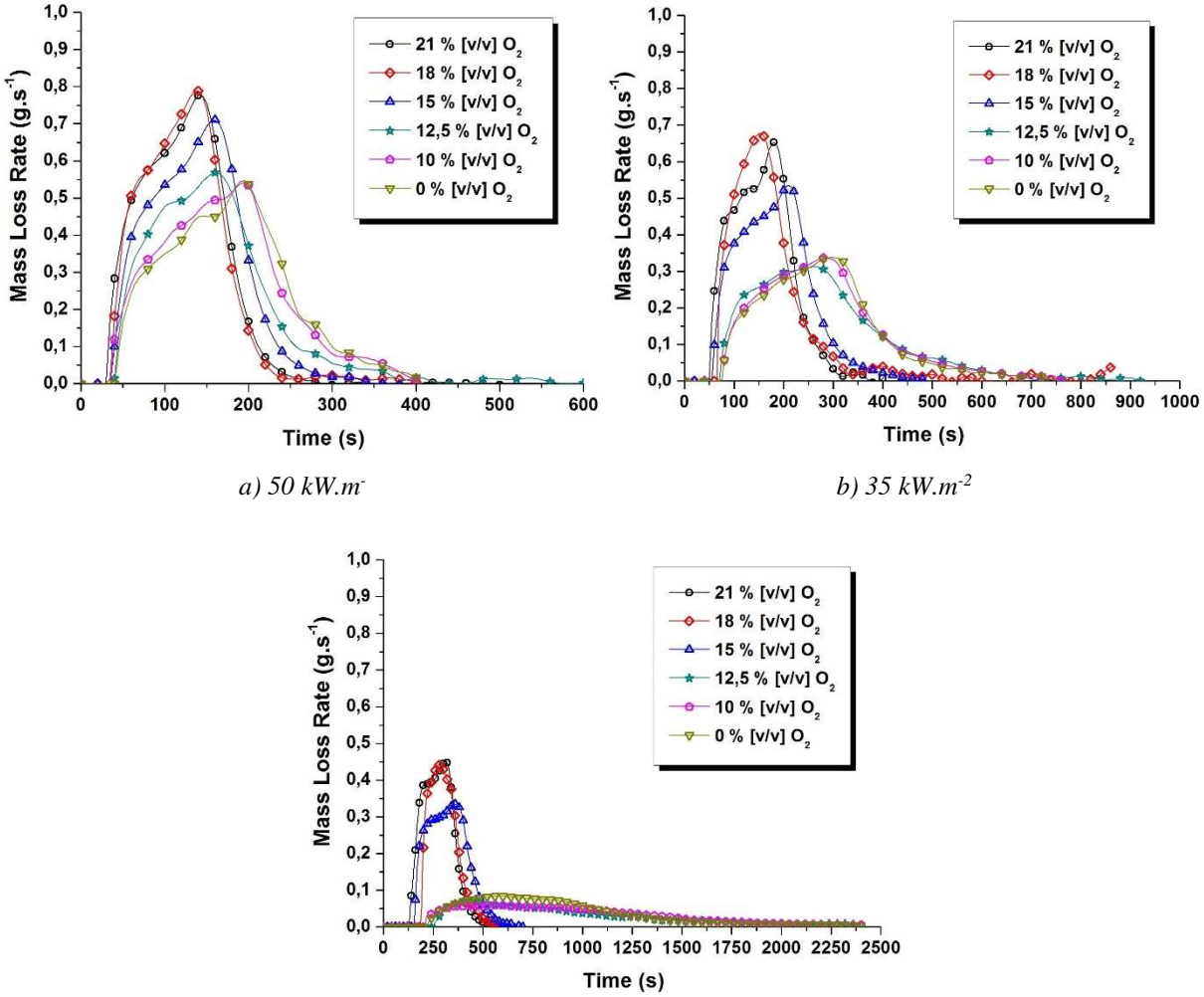

a) 50 kW.m-

b) 35 kW.m^{-2}

c) 20 kW.m^{-2}

Figure 8 : Mass Loss Rates of the ABS material for different oxygen concentrations and irradiance levels

Concerning the irradiance level, it can be seen when comparing results illustrated by Figure 8 *a)*, *b)* and *c)* that as the heat flux imposed at the surface material is reduced, the decomposition kinetic is also reduced (maximum MLR reached value, decomposition time).

Then, reducing the oxygen concentration also has a significant impact on the decomposition kinetics. As mentioned before, a combustion process hasn't been observed in all the tested conditions. When comparing for a specific irradiance level, the different curves obtained show that the reduction of the oxygen concentration has an important impact on the combustion regime.
Indeed, we can clearly see on Figure 8 *a)* that the three previously described combustion regimes can be found again. On the curves that represents the decomposition kinetics for 21 and 18% [v/v] oxygen concentration, there is no significant difference observed. The oxygen concentration in the enclosure is high enough not to disturb the combustion process and thus, does not modify the characteristics of the flame (height, temperature, chemical composition) which radiates with the same amount of energy in the two considered cases. The heat flux quantity received at the surface material, which is a combination of both the cone calorimeter heat flux, the flame heat flux (See Eq. 1 from Tewarson [39]) and the radiosity, remains approximately the same.

$$\dot{m}'' = \frac{\dot{q}_e'' + \dot{q}_{fr}'' + \dot{q}_{fc}'' - \dot{q}_r''}{\Delta H_g} \quad \text{(Eq. 1)}$$

Where:

$\dot{m}''$: Mass Loss Rate per unit area in a steady state ($g.m^{-2}.s^{-1}$)
$\dot{q}_e''$: Radiative heat flux imposed by the cone calorimeter ($kW.m^{-2}$)
$\dot{q}_{fr}''$: Radiative heat flux from the flame ($kW.m^{-2}$)
$\dot{q}_{fc}''$: Convective heat flux from the flame ($kW.m^{-2}$)
$\dot{q}_r''$: Radiosity ($kW.m^{-2}$)
ΔH_g: Heat of gasification ($kJ.g^{-1}$)

When reducing the oxygen concentration to 15%, the decomposition kinetics is slightly modified, which means that combustion efficiency has been reduced due to the local lack of oxygen. Indeed, the characteristics of the flame are modified and its radiative potency is lowered. This trend can also be verified for the results obtained at 12.5% [v/v] oxygen concentration. In this specific case, the flaming process does not occurs at the surface of the material but in the chimney and the thermal feedback imposed by the presence of the flame only has a slight impact on the total heat received at the surface of the material.
Finally, when reducing the oxygen concentration below 12.5% [v/v] (*i.e.* for cases where a non-flaming decomposition process is observed: 10 and 0% [v/v]), the decomposition kinetics is again reduced and reaches a minimum.
This analysis can be transposed to the other studied irradiance level, right down to the last detail: the behaviour when the concentration is equal to 12.5% [v/v] which is different at 50 $kW.m^{-2}$ comparing to 35 and 20 $kW.m^{-2}$. Indeed, as mentioned before, when the energy is high enough and for this specific condition of oxygen concentration, a combustion process can occur in the chimney because the temperature within is high enough to ignite the gaseous mixture. However, when reducing the imposed heat flux at the surface material, the temperature within the chimney is also reduced and the conditions for the mixture to ignite in are not reached. Then, it can be seen that the curves observed for 12.5% [v/v] oxygen concentration and for irradiance levels of 35 and 20 $kW.m^{-2}$ are similar to the ones observed for 10 and 0% [v/v] oxygen concentrations.

This analysis highlights the influence of the oxygen concentration in the decomposition environment on the combustion process (*i.e.* on the gaseous phase). Oxygen concentration in the local decomposition environment seems not to have an influence on the decomposition process occurring in the condensed phase for this specific material. Indeed, no differences on the decomposition kinetics are observed in comparison to the specific heat flux conditions where combustion process does not occur (*i.e.* shape of curves, maximum MLR reached value remains the same).
As a result, the differences observed between the mass loss rates considering a specific heat flux and varying the oxygen concentration are due to the radiative impact from the flame.

Further investigations are in progress to highlight this last point in measuring experimentally the radiative impact of the flame at the surface of the ABS material.
At last, and to echo to the previous part describing the combustion regimes, the observed and analyzed trends can be found back on Figure 9 *a)*, *b)* and *c)*, which present for all the experimentally tested conditions, the max MLR reached during the decomposition process.

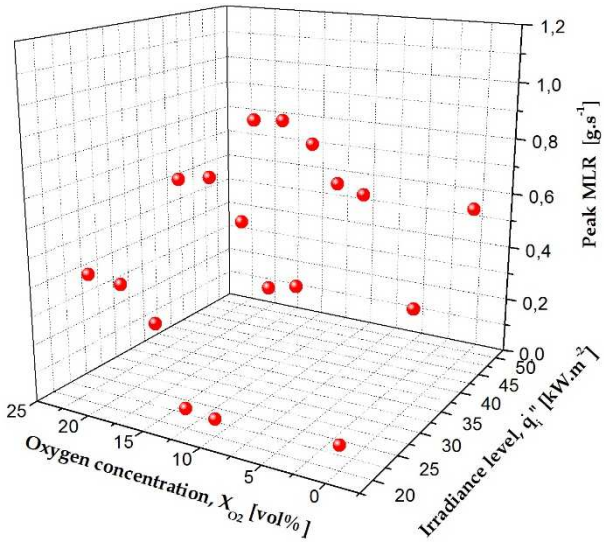

a) Peak mass loss rate as a function of the oxygen concentration and the irradiance level

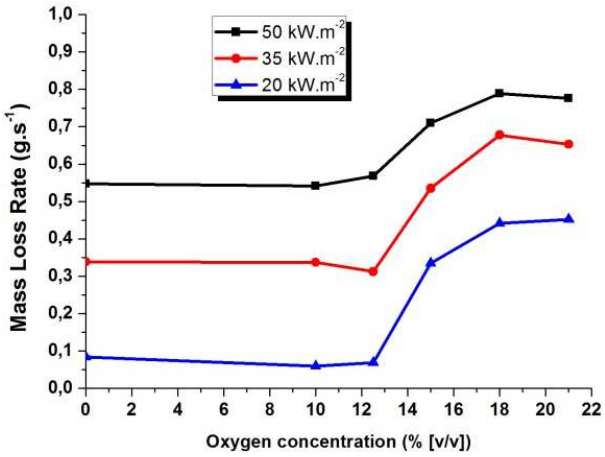

b) Mass loss rate as a function of the oxygen concentration

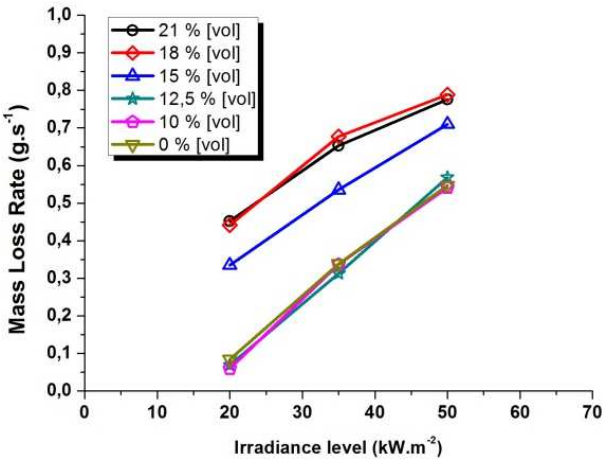

c) Mass loss rate as a function of the irradiance level

Figure 9: Maximum MLR reached for each condition tested with CACC

These figures allow the determination of the effect of the two factors (oxygen concentration and heat flux) on the MLR of the ABS material. They also highlight visually the transition between well and under-ventilated conditions that is characterized by the adjunction to the decomposition process of a flaming combustion process. This transition is achieved around 12.5 % [v/v] O_2.

Heat release rate

Results of heat release rate measurement are plotted as function of irradiance levels in Figure 10 and as function of oxygen concentration in Figure 11.

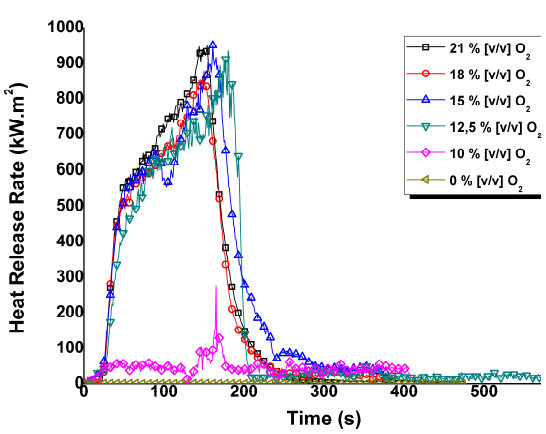

a) 50 kW.m^{-2}

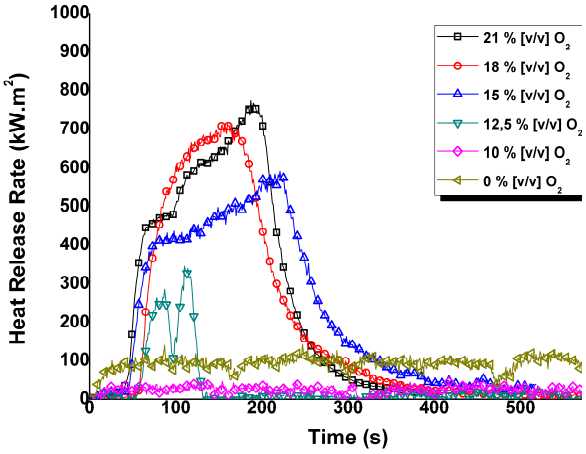

b) 35 kW.m^{-2}

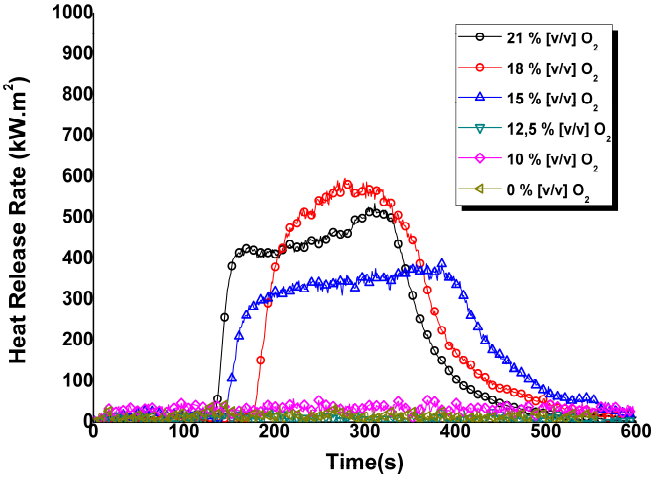

c) 20 kW.m^{-2}

Figure 10: Heat release rate vs. time as function of oxygen concentration for various irradiance levels levels

For an irradiance of 50 kW/m² (Figure 10 *a)*), results highlight a similar combustion behaviour from 21% [v/v] down to 15 % [v/v] oxygen fraction. Heat release rate curve is slightly modified at 12.5 % [v/v] of oxygen. No heat release is observed below 12.5 %. However, Figure 8 *a)* highlighted a significant mass loss rate in similar conditions, with a quite identical shape at 10 % [v/v] and 0% [v/v] of oxygen. It means that the material decomposes and produces gaseous fuel, but the oxygen quantity is not sufficient for the mixture to ignite under 12.5 % [v/v] of oxygen concentration in the volume of controlled atmosphere. The critical concentration of oxygen needed for combustion is between 12.5 and 10 % [v/v] at 50 kW/m².

For an irradiance level of 35 kW/m² (Figure 10 *b)*), the heat release curve is modified at 15%, due to mixture effects. Heat release rate curves observed at 21, 18 and 15 % [v/v] O_2 are coherent with the mass loss rate curve of Figure 8 *b)*. Below, at 12.5 % [v/v] O_2, only short heat release rate peaks are observed, corresponding to non-sustained condition and deviating from the observations on mass loss rate. This has already been mentioned in the section dealing with ignition. The critical concentration of oxygen needed for combustion is close to 12.5 % [v/v] at 35 kW/m².

For an irradiance level of 20 kW/m² (Figure 10 *c)*), no combustion is observed under 15% [v/v] of oxygen, and heat release rate curves obtained at 21, 18 and 15 % [v/v] O_2 fit well with mass loss rate

curves of Figure 8 *c)*. The critical concentration of oxygen needed for combustion is between 15 and 12.5 % [v/v] at 20 kW/m².

Figure 10 *a)* and *b)* illustrate that a positive HRR value has been quantified for a 0 % [v/v] oxygen concentration. However, it is not a relevant result and the evolution of the HRR that can be seen on the curves is a bias that can be attributed to the oxygen depletion based HRR calculation methodology and to the fact that the gaseous compounds are sampled after being mixed with ambient air as explained in the gas analysis section.

Figure 11 presents the same results, but for each oxygen concentration in the oxidizer flow, as function of irradiance level. Combustion relations between various irradiance levels are slightly affected in the range 21-15 % [v/v] of oxygen (Figure 11 *a)* to Figure 11 *c)*). 12.5 % [v/v] of oxygen represents the transition region (Figure 11 *d)*). No combustion occurs at 10 % [v/v] (Figure 11 *e)*) or below.

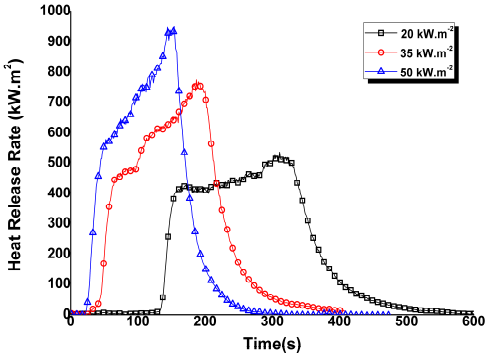

a) 21 % [v/v]

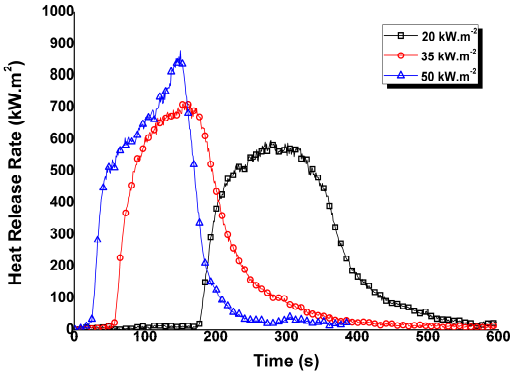

b)18 % [v/v]

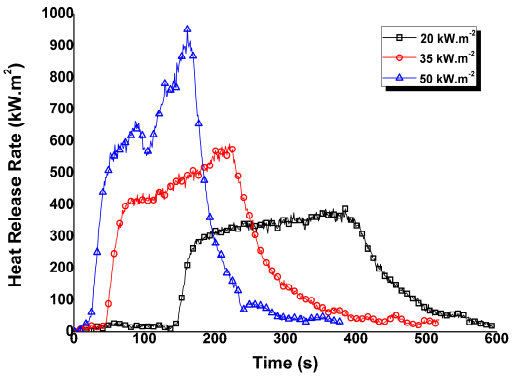

c) 15 % [v/v]

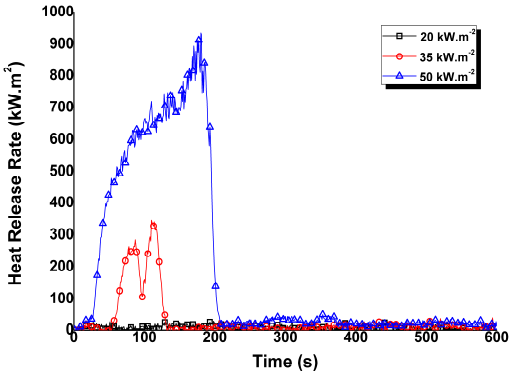

d) 12.5 % [v/v]

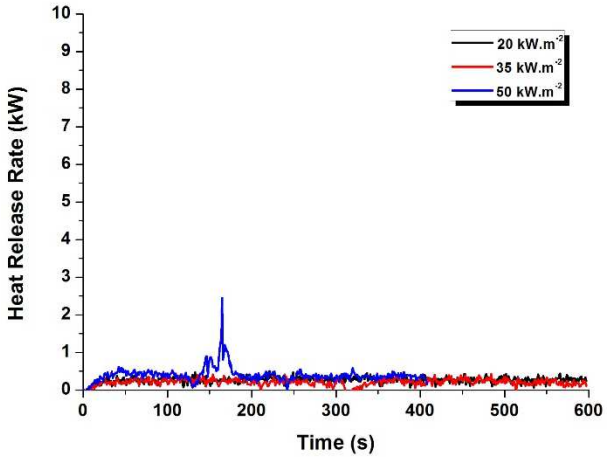

e) 10 % [v/v]

Figure 11: Heat release rate vs. time as function of irradiance levels for various oxygen concentration. Results at 0% O_2 are not significant and are not reproduced.

Figure 10 and Figure 11 highlight that the possibility of combustion in CACC is not only linked to the oxygen concentration within the enclosure but also to the energy transmitted to the surface of the material.

Gaseous emissions

Gaseous emissions have been qualified and quantified thanks to FTIR for each of the tests performed. The CO and CO_2 production yields plotted here are the one determined by the FTIR apparatus. Those components have also been quantified using the Horiba PG 250 gas analyzer. Note that the agreement of the measures between the two apparatus is very good, with differences less than 2%. Production yields for each gaseous species for which quantification limits has been achieved are presented hereafter (Figure 12). The following species are thus excluded from the analysis: Formaldehyde (H_2CO), Hydrogen Chloride (HCl), Nitrogen Dioxide (NO_2), Nitrogen protoxide (N_2O) and Sulphur dioxide (SO_2).

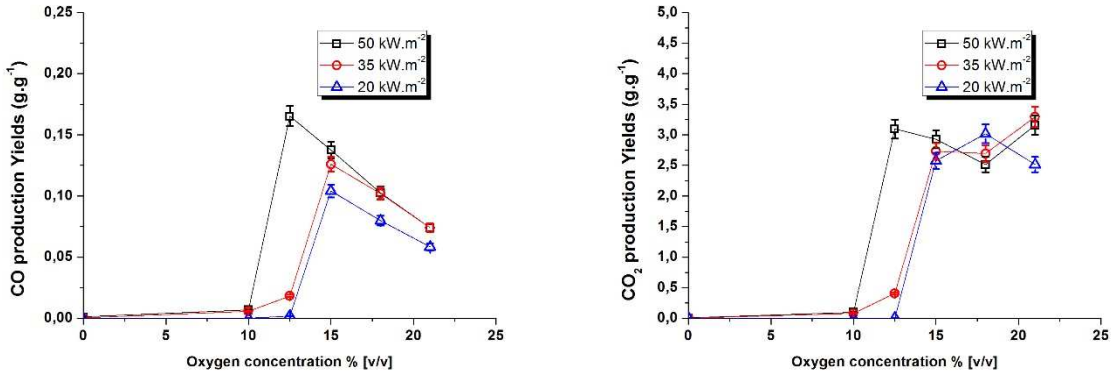

a) Carbon monoxide *b) Carbon dioxide*

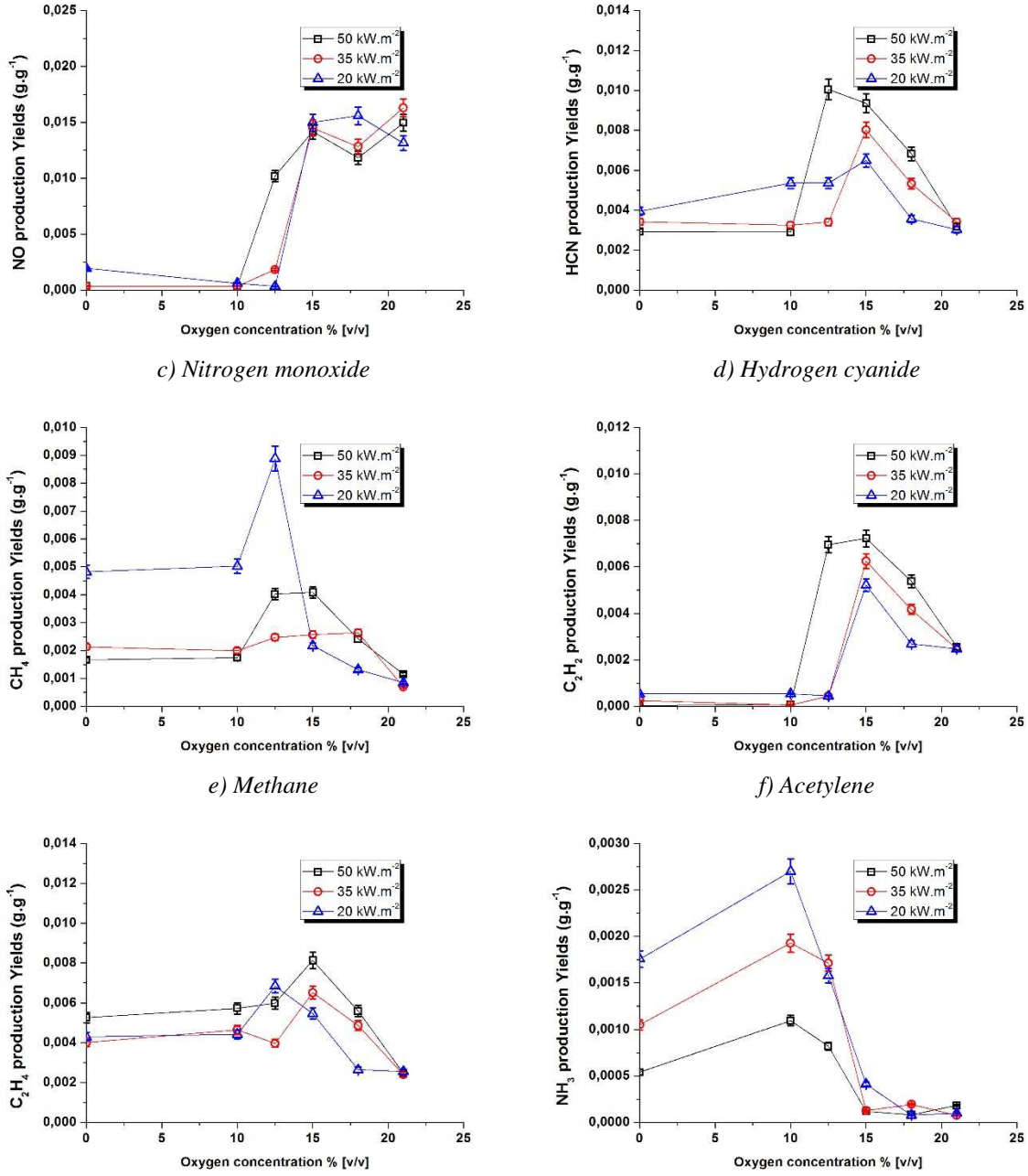

c) Nitrogen monoxide *d) Hydrogen cyanide*

e) Methane *f) Acetylene*

g) Ethylene *h) Ammonia*

Figure 12: Production Yields of different gases quantified using FTIR for several test conditions for ABS material

These results give an overview of the species emitted during the decomposition process of the ABS material. Except for CO and CO_2 emitted gaseous quantities are low regardless of the test conditions. Indeed, as the yields for CO and CO_2 reach respectively 3.25 $g.g^{-1}$ (condition 35 $kW.m^{-2}$ – 21 % [v/v] O_2) and 0.165 $g.g^{-1}$ (condition 50 $kW.m^{-2}$ – 12.5 % [v/v] O_2), other gaseous compounds are a minority.

Regardless of the specie considered (except for CO and CO_2), the emitted quantities are very low. The main gaseous compounds which participate to the combustion phenomenon have not been caught using FTIR (see CH_4, C_2H_2, C_2H_4 quantities emitted regardless of the conditions studied).
During a combustion process, it is usual to observe important emissions of CO and CO_2. Indeed, the gaseous species emitted during the decomposition process (especially the hydrocarbons) participate to the combustion phenomenon and are oxidized within the flame to form CO which will subsequently be oxidized to form CO_2. Following this logic, the emissions of hydrocarbons should be far higher

when the development of the flame is impossible within the enclosure of the CACC (when the oxygen concentration is lower than 15 or 12 % [v/v] depending on the irradiance level). However, regarding the quantities of methane, ethylene and acetylene that quantified using the FTIR, these do not rise as the oxygen concentration does not allow the appearance of a flame. Thus, it is reasonable to think that these compounds are not primary emitted species but secondary products from the decomposition of heavier species within the flaming area. It can be assumed that these heavier species can be the three monomer components of the terpolymer ABS: acrylonitrile, butadiene and styrene. Indeed, these three gaseous compounds are flammable and highly reactive. Even if they are not calibrated for quantification by the FTIR used, this point can't be directly proven by the gaseous analysis presented here, the evolution of CO and CO_2 concentrations measured can support this hypothesis. Indeed, it can be seen on Figure 13 which presents the total measured quantities of the previously selected gaseous compounds (same as on Figure 12) that there is a massive production of CO_2, notwithstanding is a restrained production of hydrocarbons. Knowing that the matrices of acrylonitrile, butadiene and styrene are composed exclusively of carbon and hydrogen, this explains the origin of the massive CO_2 production. Indeed, once these three compounds are oxidized during the flaming process, carbon monoxide is formed and then oxidized to form carbon dioxide.

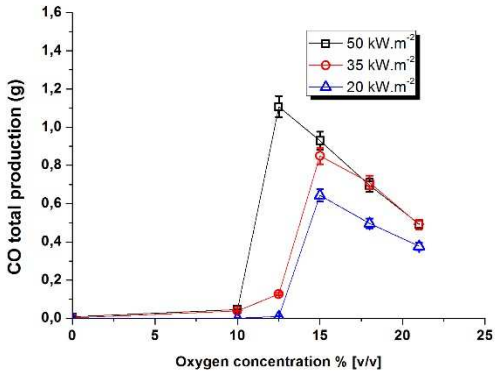

a) Carbon monoxide

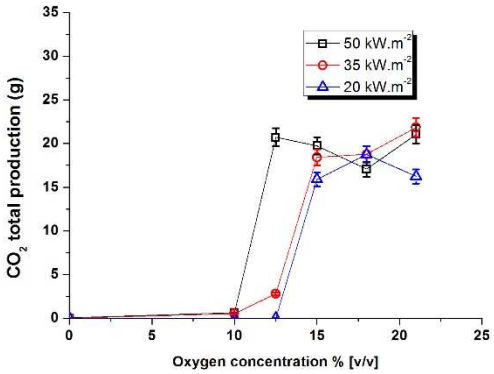

b) Carbon dioxide

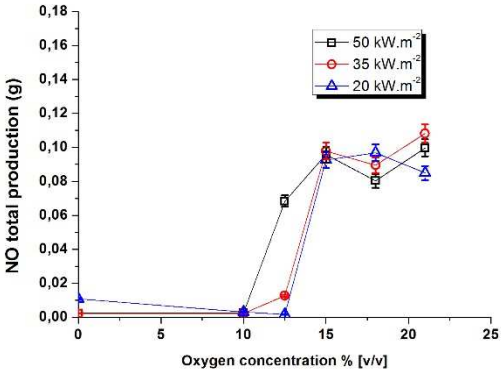

c) Nitrogen monoxide

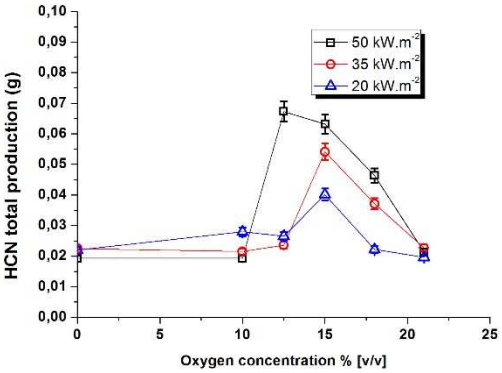

d) Hydrogen cyanide

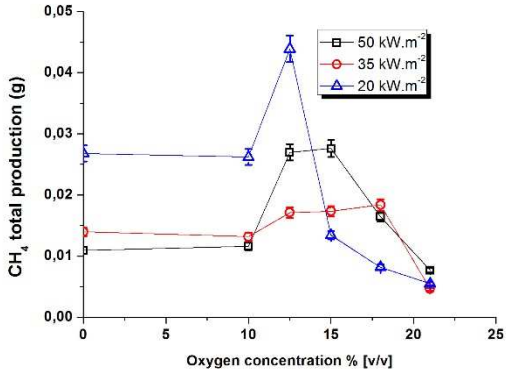

e) Methane

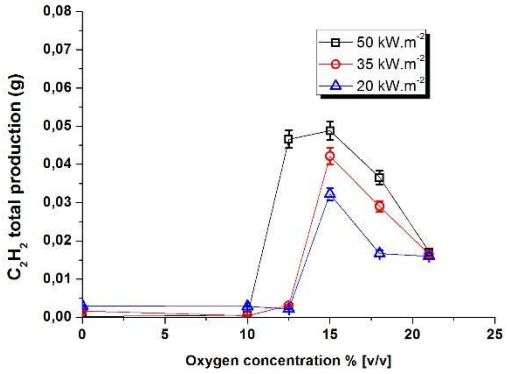

f) Acetylene

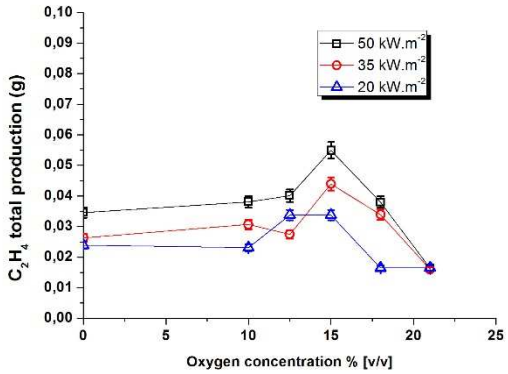

g) Ethylene

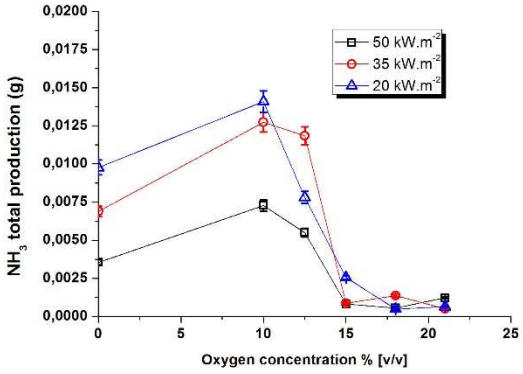

h) Ammonia

Figure 13 : Total production of different gases quantified using FTIR for several test conditions for ABS material

Although the evolution of gaseous emissions of the different compounds is interesting, this is not the main topic of the presented work. This part is then restrained to the study of the evolution of the main gaseous compounds: CO and CO_2 because their evolution can provide useful information concerning decomposition and combustion regimes.

Regarding the maximum quantities of CO and CO_2, a detailed analysis is presented hereafter in focusing on the temporal evolution of the emissions of these two gaseous compounds (see Figure 14).

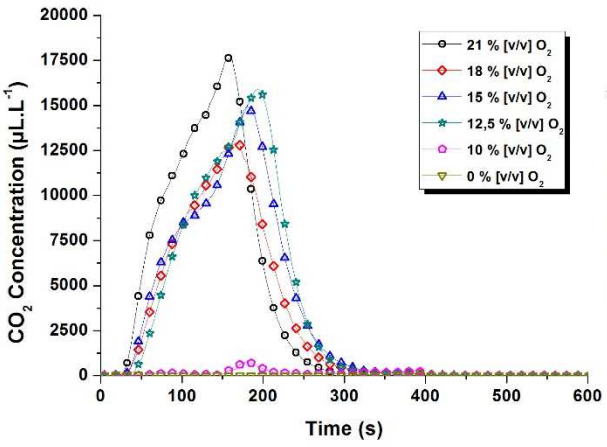

a)

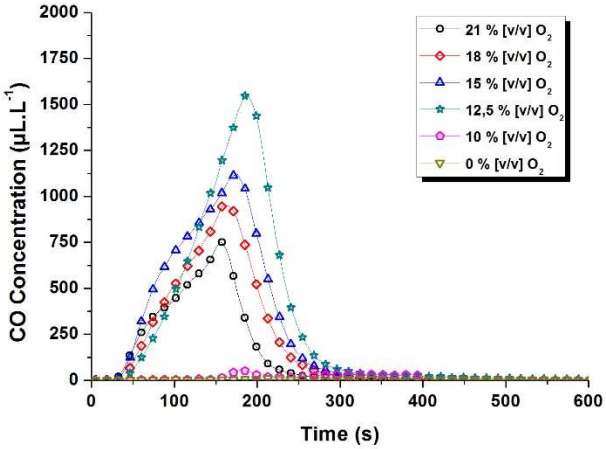

d)

50 kW.m^{-2}

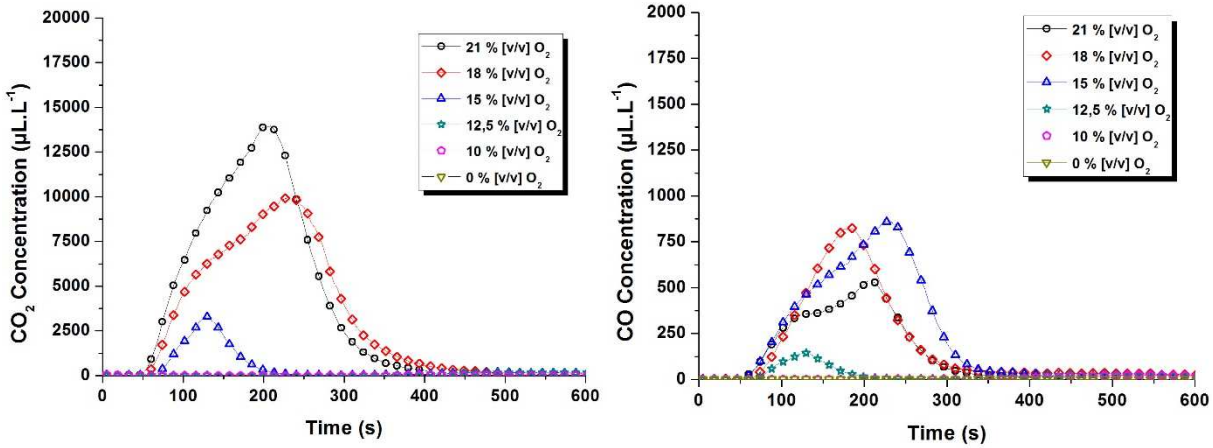

b) e)

35 kW.m^{-2}

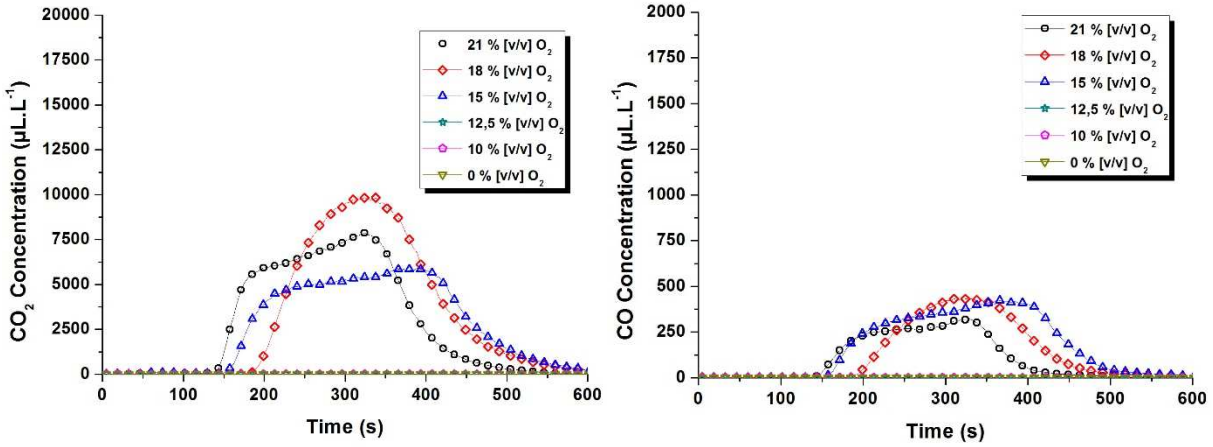

c) f)

20 kW.m^{-2}

Figure 14: Evolution of the CO_2 and CO concentrations in the different decomposition conditions tested

It would be inappropriate here to perform a precise analysis of the CO and CO_2 emissions regarding the quantification. Indeed, it must be noted that the sampling point is located downstream of the decomposition enclosure and thus the gaseous compounds that emerge from the chimney are diluted in ambient air before reaching the sampling point. Thereby, gaseous effluents from the decomposition process or from the combustion (when allowed by the oxygen concentration) may continue to oxidize before reaching the sampling point. Nonetheless, the dilution factor is always the same (even if there could be a slight difference because of the different smoke temperatures function of the fixed irradiance level), and thus the evolution of the emitted quantities of CO and CO_2 can be compared to provide information that can confirm the previously mentioned hypotheses concerning the decomposition regimes.

As shown on Figure 14 a) for 50 kW.m^{-2} irradiance level, the quantity of emitted CO_2 is similar for all the conditions for which a combustion process (regardless its location *e.g.* on the surface of the sample or within the chimney) in the gaseous phase is associated with the decomposition of the condensed phase (*i.e.* 21, 18, 15, and 12.5 % [v/v]). Although different decomposition regimes can be encountered when diminishing the oxygen concentration within the enclosure, CO_2 concentrations are not drastically affected.
This observation is not true for the other irradiance levels presented (see Figure 14 *b)* and *c)*) and the diminution of the oxygen concentration within the enclosure implies a diminution of the CO_2

emissions. This trend is particularly observable for an irradiance level of 35 kW.m^{-2} and can also be verified at 20 kW.m^{-2} except for the curve that corresponds to the test where the oxygen concentration has been fixed to 18 % [v/v] (this result can be attributed to an experimental bias as it does not follow the classically observed trend for the other irradiance levels).

When the oxygen concentration is equal to 15% [v/v], the concentration of emitted CO_2 is lower than the ones observed for 21 and 18% [v/v]. In this burning condition, the oxygen concentration starts to be a limiting factor and even if the concentration is high enough to ensure combustion, it is not to wholly oxidize CO into CO_2. This last point can be proven in focusing on the CO emissions. Indeed on Figure 14 *d)*, *e)* and *f)* it can be seen that reducing the oxygen concentration in the enclosure has the effect of increasing the carbon monoxide concentrations.

For the 12.5% [v/v] oxygen concentration condition, it can be noticed that at 35 kW.m^{-2}, there is still an important emission of CO_2 and CO, although it is considerably reduced comparing to the ones presented for 21, 18 and 15% [v/v] oxygen concentration conditions. In this specific condition, combustion requirements are reached locally under the form of flash point near the pilot flame. Thus, a part of the gaseous compounds emitted during the decomposition are oxidized at this point but in quantities that are quite low. This phenomena is directly linked to the energy received at the surface material and does not occur when this energy is too low. This specific behaviour cannot be observed on Figure 14 *c)* when the irradiance level is fixed to 20 kW.m^{-2}.

Reducing the oxygen concentration within the enclosure inhibits the CO_2 production. As CO_2 is formed by the oxidation of CO, even if the oxygen concentration within the enclosure is high enough to allow the flame to appear and sustain, its rarefaction acts like a brake to the formation of CO_2. In order to confirm these hypotheses, Figure 15 presents the CO/CO_2 ratios for each analyzed conditions.

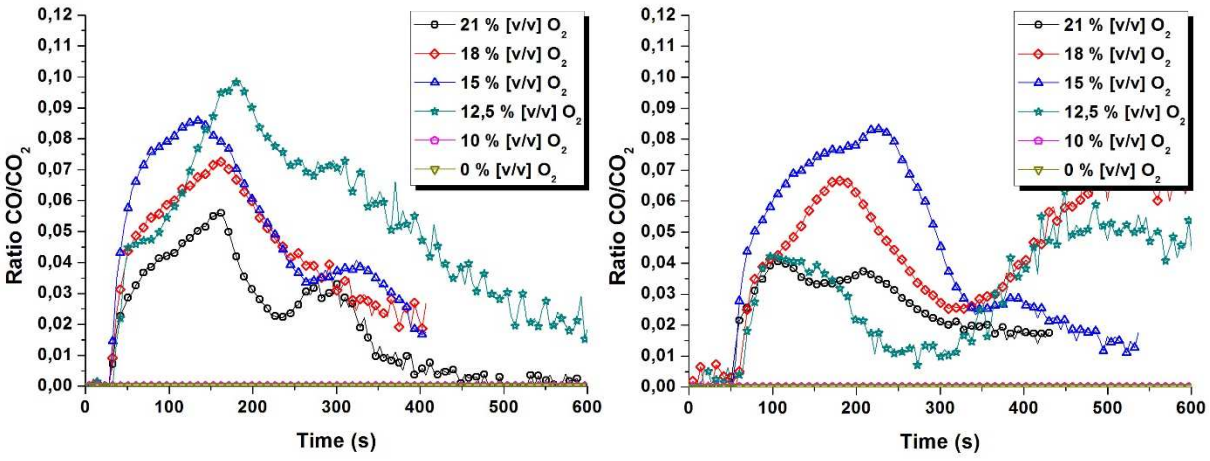

a) 50 kW.m^{-2} b) 35 kW.m^{-2}

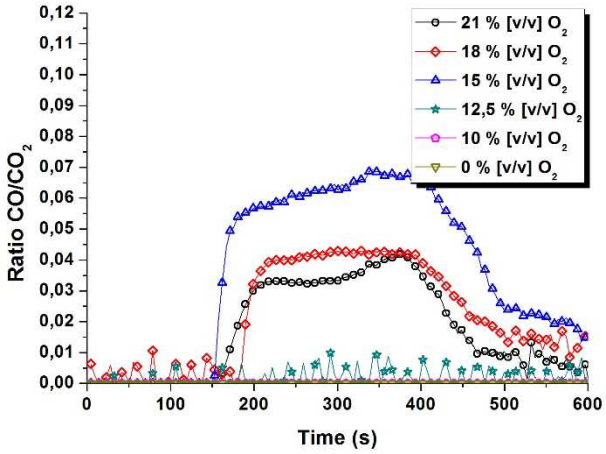

c) 20 kW.m^{-2}

Figure 15: CO/CO2 ratios for the ABS material for the different irradiance levels

Results observed on Figure 15 confirms the previous affirmations. Indeed, regardless of the studied condition, the lower the oxygen concentration in the enclosure, the higher the values of the CO/CO_2 ratios. This ratio is thus an excellent indicator to describe the combustion efficiency. The higher the ratio, the lower the possibility for CO to react with oxygen to form CO_2 within the flaming area. As a consequence, when the CO/CO_2 ratio increases, the energy provided by the flame decreases.

This analysis completes the hypothesis emitted in the previous sections on the fire behaviour of the material and especially on the combustion regimes that can be encountered using the CACC when studying an ABS material.

CONCLUSION

A complete assessment of the thermal decomposition of the ABS material have been carried out using the controlled atmosphere cone calorimeter coupled to a Fourier Transform Infrared spectrometer. Most important parameters classically studied using cone calorimeter have been presented in order to determine the effect of both the irradiance level imposed at the surface of the material and the oxygen concentration, on reaction to burning of the material. These two specific parameters are the main ones that can modify, in enhancing or reducing the decomposition kinetics, the thermal behaviour of a material when exposed to fire.
The present study has notably proven that different combustion regimes, that have to be known to describe the nature of a well or under-ventilated fire, can be described in cross-linking the results obtained for the mass loss rate, the heat release rate and the carbon monoxide and dioxide concentrations.
The determination of decomposition regimes is an important challenge. Their limits depend on three factors: the concentration of combustible gas, the concentration of ambient oxygen and the energy required to initiate the flaming combustion. Three key parameters, representative of fires in under-ventilated confined environments. However, they also depend on the scale of the study and the type of equipment used (in this case the CCAC). Indeed, even if the concentration of ambient oxygen can allow the appearance of a flame, the amount of pyrolysis gas available is also a limiting factor as are the mixing conditions of these two elements. This last point explains why the boundary of decomposition zones cannot be fixed definitely and extrapolated on a larger scale. The results, although highlighting phenomena likely to occur on a real scale, must therefore be analyzed in detail before being transposed to a higher scale.

Experiments indicate, as expected, that the irradiance applied to the surface of the samples is of particular importance. It is the main factor of the phenomenon of thermal decomposition. Its increase

leads to a significant variation in the kinetics of decomposition of the materials. Moreover, the high values of irradiance (50 and 35 $kW.m^{-2}$) allow phenomena to occur in the gas phase that are not observed for lower values of irradiance (20 $kW.m^{-2}$). It is possible to assume that the irradiance imposed at the surface of the samples is representative of a real fire, but it should be borne in mind that in a real fire situation, the energy balance received at the surface of a material is the sum of all modes of heat transfer present in the decomposition environment. All these modes of transfer are not taken into account independently when using the cone calorimeter (convection in particular which can act as an increasing of reducing factor to the energy balance at the surface of the material). However, the phenomena observed thanks to the cone calorimeter tests occurring in the transition zone between a well-ventilated and under-ventilated environment may, in all likelihood, occur on a real scale. In this perspective, it is important to take into account the energy variations that can cause these phenomena.

The effect of the oxygen concentration on the decomposition of the ABS material studied indicates that this parameter plays a major role in the establishment of the flaming combustion process but does not affect the thermal decomposition of the solid phase. This observation is however limited to this material and to the testing conditions presented in this study.

From this global analysis, as perspectives, emerges the necessity to quantify two primordial factors having an impact on the surface thermal balance during the thermal decomposition of the material: The influence of the flaming process on the energy balance at the surface and in depth of the material and the impact of the oxygen concentration on the decomposition process for materials in solid phase can be affected by oxygen.

ACKNOWLEDGMENTS

The authors thank the following for the financial, technical and human support:
The Centre d'Etude des TUnnels (CETU)
The Laboratoire National de métrologie et d'Essais (LNE)
The Institut des Risques Industriels Assurantiels et Financiers (IRIAF)
This work pertains to the French Government program "Investissements d'Avenir" (LABEX INTERACTIFS, reference ANR-11-LABX-0017-01).

REFERENCES

[1] ISO/TS 5660-5:2020, Reaction-to-fire tests — Heat release, smoke production and mass loss rate — Part 5: Heat release rate (cone calorimeter method) and smoke production rate (dynamic measurement) under reduced oxygen atmospheres

[2] G. Mulholland, M. Janssens, S. Yusa, W. Twilley, V. Babrauskas, The Effect Of Oxygen Concentration On Co And Smoke Produced By Flames, Fire Saf. Sci. 3 (1991) 585–594.

[3] R.V. Petrella, N. Batho, The controlled atmosphere cone calorimeter - an improved tool for fire testing of materials, Proc. 1st Int. Conf. Fire Mater. San Fr. USA. (1992) 311–321.

4 J. Hitaniemi, R. Kallonen, E. Mikkola, Burning Characteristics of selected substances: Production of Heat, Smoke and Chemical species, Fire Mater. 23 (1999) 171–185.

[5] M. Werrel, J.H. Deubel, S. Krüger, A. Hofmann, E. Antonatus, U. Krause, F. Deuerler, Use and benefit of a controlled atmosphere cone calorimeter, Proc. Thirteen. Int. Conf. Fire Mater. San Fr. USA. (2013) 273–285.

[6] C. Gomez, M. Janssens, A. Zalkin, Using the Cone Calorimeter for quantifying toxic potency, Proc. 12th Int. Fire Sci. Eng. Conf. (Interflam), Fire Saf. Proceedings, Nottingham. (2010).

[7] D. Marquis, F. Hermouet, E. Guillaume, Effects of reduced oxygen environment on the reaction-to-fire of a poly-(urethane-isocyanurate) foam, Fire Mater. - Artic. Available Online. (2015). doi:10.1002/fam.2378.

[8] Project ISO/CD TS 21397.2, FTIR analysis of fire effluents in cone calorimeter tests (Accessed August 2020)

[9] J. Vandome, Poly(styrène/butadiène/acrylonitrile) ABS, Tech. l'Ingénieur - [Archives] Plast. Compos. - a3345. (1978).

[10] H. Ma, L. Tong, Z. Xu, Z. Fang, Y. Jin, F. Lu, A novel intumescent flame retardant: Synthesis and application in ABS copolymer, Polym. Degrad. Stab. 92 (2007) 720–726.
[11] H. Ma, L. Tong, Z. Xu, Z. Fang, Intumescent flame retardant-montmorillonite synergism in ABS nanocomposites, Appl. Clay Sci. 42 (2008) 238–245.
[12] M. Suzuki, C. a. Wilkie, The thermal degradation of acrylonitrile-butadiene-styrene terpolymei as studied by TGA/FTIR, Polym. Degrad. Stab. 47 (1995) 217–221.
[13] M.P.L. di Cortemiglia, G. Camino, L. Costa, M. Guaita, Thermal degradation of ABS, Thermochim. Acta. 93 (1985) 187–190.
[14] H. Ma, J. Wang, Z. Fang, Cross-linking of a novel reactive polymeric intumescent flame retardant to ABS copolymer and its flame retardancy properties, Polym. Degrad. Stab. 97 (2012) 1596–1605.
[15] P. Song, Z. Cao, S. Fu, Z. Fang, Q. Wu, J. Ye, Thermal degradation and flame retardancy properties of ABS/lignin: Effects of lignin content and reactive compatibilization, Thermochim. Acta. 518 (2011) 59–65.
[16] J. Rutkowski, B. Levin, Acrylonitrile–butadiene–styrene copolymers (ABS): Pyrolysis and combustion products and their toxicity—a review of the literature, Fire Mater. 10 (1986) 93–105.
[17] ISO 5660-1, Reaction to fire tests - Heat release, smoke production and mass loss rate - Part 1: Heat release rate (cone calorimeter method), (2015 + AMD1:2019).
[18] ISO 291, Plastics - standard atmospheres for conditioning and testing, (2005).
[19] ISO 5725-1, Accuracy (trueness and precision) of measurement and results, (1994).
[20] F. Hiesch, H. Beeson, D. Harolds, Cone Calorimeter testing of Epoxy/Fiberglass and Brominated Epoxy/Fiberglass Composites in standardal and oxygen-enriched environments, ASTM Spec. Tech. Publ. 1267. 3 (1995) 152.
[21] J.E. Leonard, P.A. Bowditch, V.P. Dowling, Development of a controlled-atmosphere cone calorimeter, Fire Mater. 24 (2000) 143–150. doi:10.1002/1099-1018(200005/06)24:3<143::AID-FAM728>3.0.CO;2-L.
[22] D. Marquis, E. Guillaume, A. Camillo, M. Pavageau, T. Rogaume, Usage of Controlled Atmosphere Cone Calorimeter to provide input data for toxicity modelling, Proc. 12th Int. Conf. Fire Mater. San Fr. USA. (2011).
[23] M. Werrel, J. Deubel, S. Krüger, A. Hofmann, U. Krause, The calculation of the heat release rate by oxygen consumption in a controlled-atmosphere cone calorimeter, Fire Mater. 38 (2014) 204–226.
[24] D. Marquis, E. Guillaume, D. Lesenechal, Accuracy (trueness and precision) of cone calorimeter tests with and without a vitiated air enclosure, Proc. Ninth Asia-Oceania Symp. Fire Sci. Technol. 62 (2013) 103–119.
[25] ISO 13927: Plastics-Simple Heat Release Test using a Conical Radiant Heater and a Thermopile Detector, (2015).
[26] ISO 5660-3, Reaction to fire tests - Heat release, smoke production and mass loss rate - Part 3: Guidance on measurements, (2012).
[27] C. Hugget, Estimation of rate of heat release by means of oxygen consumption measurements, Fire Mater. 12 (1995) 1980.
[28] M.L. Janssens, Measuring rate of heat release by oxygen consumption, Fire Technol. 27 (1991) 234–249.
[29] M. Janssens, W. Parker, Oxygen consumption calorimeter, Heat Release Fires, Babruaskas, V., Grayson S., Ed. London, Edt Elsevier. 3 (1992) 31–59.
[30] W. Thornton, The relation of Oxygen to the Heat of Combustion of Organic Compounds, Philos. Mag. 3 (1917) 196–203.
[31] ISO 19702, Toxicity testing of fire effluents - Guidance for analysis of gases and vapours in fire effluents using FTIR gas analysis, (2015).
[32] P. Fardell, E. Guillaume, Sampling and measurments of toxic fire effluents, Fire Toxic. - Chapter 11. Woodhead Publ. Mater. ISBN 9781-84569-502-6. (2010).
[33] Y. Le Tallec, E. Guillaume, Fire gases and their chemical measurmements, Hazard Combust. Prod. Intersci. Commun. ISBN 978-0-955 6548-2-4. (2008) 43–58.
[34] E. Guillaume, L. Saragoza, Application of FTIR analyzers to fire gases - progress in apparatus

and method validation for quantificative analysis, 14th Int. Conf. Fire Mater. San Fr. United States. (2015).
[35] E. Guillaume, L. Saragoza, K. Wakatsuki, P. Blomqvist, Effect of gas cell pressure in FTIR analysis of fire effluents, Fire Mater. 39 (2014) 675–684.
[36] A. Tewarson, Generation of heat and gaseous, liquid and solid products in Fire, SFPE Handb. Fourth Ed. - Chapter 3-4 - ISBN 978-0-87765-821-4, 2013.
[37] L. Spadaccini, M. Colket, Ignition delay characteristics of methane fuels, Progresse Energy Combust. Sci. 20 (1994) 431–460.
[38] J.E.J. Staggs, Savitzky-Golay smoothing and numerical differentiation of cone calorimeter mass data, Fire Saf. J. 40 (2005) 493–505. doi:10.1016/j.firesaf.2005.05.002.
[39] A. Tewarson, J.L. Lee, R.F. Pion, The influence of oxygen concentration on fuel parameters for fire modeling, Proc. Eighteenth Symp. Combust. 18 (1981) 563–570.